Digital Pathology Image Reconstruction with Alternating Direction Method of Multipliers using Wavelet, Contourlet and Shearlet Transforms

Esra ŞENGÜN ERMEYDAN[1*], İlyas ÇANKAYA[2]

[1,2] Department of Electrical and Electronics Engineering, Faculty of Engineering and Natural Sciences, Ankara Yıldırım Beyazıt University, Ankara, Türkiye

[*1] esrasengunermeydan@aybu.edu.tr, [2] ilyas.cankaya@aybu.edu.tr

Abstract: Digital pathology refers to image-based environment in which acquisition, extraction and interpretation of pathology information is supported by computational techniques. It has a huge potential to facilitate the diagnostic process, however, big data size and necessity of large storage areas are challenging. Therefore, in this research, Compressed Sensing (CS) scheme is studied with digital pathology images in order to reduce the amount of data for reconstruction. CS requires the sparsity of signals for a successful recovery which means that different sparsifying bases can alter the final performance. Wavelet, Contourlet and Shearlet Transforms are investigated to sparsify the digital pathology images, it is seen that Contourlet Transform is superior. Alternating Direction Method of Multipliers (ADMM) is chosen for reconstruction since it is a robust and fast convex optimization method. Despite the fact that digital pathology images are less sparse than classical images, CS reconstruction is satisfactory, which emphasizes the potential of CS for digital pathology. This study can be pioneering in the field of CS with digital pathology so it can encourage further studies of CS based imaging with different type of microscopes or at different wavelengths.

Key words: Compressed Sensing, Digital Pathology, Wavelet Transform, Contourlet Transform, Shearlet Transform.

Dalgacık, Contourlet ve Shearlet Dönüşümleri Kullanılarak Çarpanların Alternatif Yön Yöntemi ile Dijital Patoloji Görüntüsü Geriçatılması

Öz: Dijital patoloji, patoloji bilgilerinin elde edilmesi, çıkarılması ve yorumlanmasının hesaplamalı tekniklerle desteklendiği görüntü tabanlı ortamı ifade eder. Teşhis sürecini kolaylaştırma açısından büyük bir potansiyele sahiptir ancak büyük veri boyutu ve geniş depolama alanlarının gerekliliği zorlayıcıdır. Bu nedenle, bu araştırmada, yeniden yapılandırma için veri miktarını azaltmak amacıyla Sıkıştırılmış Algılama (CS) şeması dijital patoloji görüntüleri ile incelenmiştir. CS, başarılı bir kurtarma için sinyallerin seyrekliğini gerektirir; bu, farklı seyrekleştirici bazların nihai performansı değiştirebileceği anlamına gelir. Dijital patoloji görüntülerini seyrekleştirmek için Dalgacık, Contourlet ve Shearlet Dönüşümleri incelenmiştir, Contourlet Dönüşümünün üstün olduğu görülmüştür. Geriçatma için Alternatif Yön Çarpan Yöntemi (ADMM) sağlam ve hızlı bir dışbükey optimizasyon yöntemi olduğundan seçilmiştir. Dijital patoloji görüntülerinin klasik görüntülere göre daha az seyrek olmasına rağmen CS geriçatması tatmin edicidir, bu da CS'nin dijital patoloji için potansiyelini vurgulamaktadır. Bu çalışma, dijital patoloji ile CS alanında öncü olabilir ve farklı tipte mikroskoplarla veya farklı dalga boylarında CS tabanlı görüntülemeye yönelik daha ileri çalışmaları teşvik edebilir.

Anahtar kelimeler: Sıkıştırılmış Algılama, Dijital Patoloji, Dalgacık Dönüşümü, Contourlet Dönüşümü, Shearlet Dönüşümü.

1. Introduction

Medical imaging is a general term for using several different technologies to view the human body or human specimens in order to diagnose, monitor, or treat medical conditions. Through medical images, the area of the human body that is invisible or too small to be observed with the naked eye can be visualized and examined. Medical images provide very important data in the treatment process. Digital pathology is a dynamic branch of medical imaging which enables the acquisition, extraction and interpretation of pathology information using a very high-resolution picture of a microscope slide containing a sample of tissue in a digital environment [1]. The collaboration and engagement of professionals from different medical institutions are facilitated by digital pathology methods. The clinicians in other locations can easily be consulted for second opinion and obviously time and cost for diagnose are saved considerably. Besides, the risks associated with physically transporting slides are eliminated. The COVID-19 pandemic's emphasis on leveraging digital infrastructure for remote patient monitoring [2] also underscored the potential of digital pathology, which can allow pathologists to analyze and diagnose disease from anywhere, improving both healthcare accessibility and efficiency. Moreover, there are lots of studies to develop automated pathology techniques to make the diagnosis less subjective and less time consuming [3]. It is estimated that the global digital pathology market size will reach USD 1.74 billion by 2030,

---

[*] Corresponding author: esrasengunermeydan@aybu.edu.tr. ORCID Number of authors: [1] 0000-0002-5953-4301, [2] 0000-0002-6072-3097

registering a CAGR of 7.5% [4]. However, digital pathology slide images are big in size and need large storage areas therefore both the storage and the transmission of pathological images for diagnosis and monitoring purposes are still challenging. One of the solutions for reducing the data is compressing the images after they are sampled at Nyquist rate [5,6]. On the other hand, the drawback of these conventional compression methods is that acquiring too much data in a fast way is hard and quite expensive due to physical constraints. Besides, there is an obvious question asking whether there is a way of getting the data which contains information directly. The efforts for answering this question have led to a novel sensing paradigm called as Compressed Sensing (CS) in 2006. CS basically claims that signals can be reconstructed with lower sampling rates than Shannon-Nyquist theorem dictates [7, 8]. In other words, the signal is compressed at the time of sensing [9] so the number of measurements for reconstruction, acquisition time and energy are reduced.

CS has applied to a wide range of areas such as astronomy, communications, signal processing and imaging beyond the visible band. It is claimed that CS has a big potential on medical imaging [10]. In fact, first application of CS was reducing the measurement time of data acquisition for MRI [11]. The technology using CS in MR imaging has been quite mature so that in 2017, FDA has approved the clinical usage of Compressed Sensing MRI [12]. It is indicated that cardiac cine imaging is reduced from 4 minutes to just 16 seconds if CS is applied to acquire the required data. In addition to MRI, compressed sensing methods are also intensively studied in medical fields such as x-ray, computed tomography, ultrasound imaging, and compression of ECG/EEG signals [10], Another application area of CS is the possibility of imaging with single-pixel architecture at different wavelenghts such as THz or infrared [13]. Advances in CCD and CMOS technology made it much easier and cheaper to obtain high resolution images in digital cameras. However, at wavelengths where silicon cannot be used, cameras are still too expensive and/or too large in size. Therefore, there is a need for inexpensive and accessible microscopes that can be used for imaging biological samples, for quality control in industry or for research in materials science. In order to satisfy this need, single pixel microscope with compressed sensing techniques has drawn attention in academia [14]. Besides, CS with different type of microscopes such as electron, fluorescence, photoacoustic and laser scanning are also promising since they reduce the measurement time and increase the quality of imaging [15–17]. In this study, compressed sensing of digital pathology images with different sparsifying transforms is considered. Wavelet, Contourlet and Shearlet Transforms are studied as sparsifying bases. Contourlet and Shearlet Transforms are multi resolution and multi scale, therefore these transforms are attractive for medical imaging applications. Alternating Direction Method of Multipliers (ADMM) [18] is selected for the reconstruction part. It is a robust convex optimization algorithm that breaks the problem into smaller pieces, each of which is easier to handle. In the previous work [19], CS based single pixel microscope configuration was studied, Gaussian and Bernoulli random matrices were used as measurement matrices, during that study it was observed that, random matrices require large storage and cause slow reconstruction. Moreover, total variation and ℓ_1 norm minimization algorithms which were used for recovery part need the inverse matrix of the sparsifying transform. However, obtaining a compact single matrix when multi resolution and multi scale transformation is not possible. Therefore, in this study, reconstruction algorithm is changed to ADMM, another outcome of this choice is the possibility of studying higher resolution images than the previous work [19]. The performance of compressed sensing of digital pathology images is compared with classical peppers image and the quality of reconstruction is evaluated using different image similarity indices such as Structural Similarity Index (SSIM) [20], Haar Wavelet-Based Perceptual Similarity Index (HaarPSI) [21] and Peak Signal to Noise Ratio (PSNR). CS scheme ensures compression during the acquisition of data therefore digital pathology images could be reconstructed using fewer data, besides this study can encourage CS based microscopic configurations beyond the visible band or with different type of microscopes.

2. Materials and Methods

2.1 Compressed Sensing

Compressed Sensing theory [7], [8] claims that if a signal is sparse or compressible, then the signal can be reconstructed using considerably less data than Shannon-Nyquist theorem states [5]. The data acquisition process can be modeled as in equation 1:

$$z = Mx \tag{1}$$

where z are measurements, M is the measurement matrix or masking operator, x is the signal that is desired to be reconstructed. In CS, the measurement matrix M is not full rank, meaning that there will be infinitely many solutions corresponding to same z due to the null space of M, so the reconstruction problem is an ill posed problem, however, these kind of problems can be solved by convex optimization methods [8], [9] thanks to the sparsity of

the signal x. The problem in Equation 1 is known to have a unique sparse solution if the masking operator M satisfies the Restricted Isometry Property (RIP) [22] which geometrically means that the projection of M preserves the geometry of the set of sparse signals. Designing a combinatorial RIP matrix is unfortunately NP hard problem; however random matrices are known to satisfy RIP with high probability [23]. Although the problem of masking operator with RIP can be solved with random matrices, another key assumption for a successful reconstruction is that the signal x should be sparse. In many real-life applications, the signal x is not directly sparse but it becomes sparse if a suitable transform is applied. For images, Wavelet Transform (WT) [24] is the most prominent sparsifying transform, it is at the heart of JPEG2000 [6] which is widely used compression scheme. On the other hand, for cartoon-like images such as digital pathological ones, multilevel and multi scale transforms like shearlets and contourlets can represent the edges and curves better that are present in the image [25], [26].

2.2 Wavelet, Contourlet and Shearlet Transforms

Wavelet Transform is generally defined as a technique in which a signal/image is analyzed in the time/spatial domain by using shifted or contracted versions of a basis function called the mother wavelet. By using a set of wavelet orthonormal basis functions constructed by Mallat and Daubechies [24], [27], [28] both the frequency and time/spatial information can be captured simultaneously. Therefore, following the introduction of wavelets, they have been applied to a diverse range of areas from seismic signal analysis to data compression, medical imaging, pattern recognition, computer graphics. Although it is used in a wide range of areas, one of the most popular applications of WT is in image processing. It specifically sparsifies the images by decomposing it in low and high frequencies. The detail parts of the image are represented by high frequencies whereas smooth parts of the images are decomposed in the low frequencies. In WT, the mother wavelet ψ is dilated and translated to form a basis for image representation. In other words, the high frequency part of image is stored in the wavelet function ψ_{jk} and the low frequency part is described by the scaling function φ, as in (2) and (3):

$$\varphi_{j,k}(x) = 2^{j/2}\varphi(2^j x - k) \tag{2}$$

$$\psi_{j,k}(x) = 2^{j/2}\psi(2^j x - k) \tag{3}$$

Scaling functions are orthogonal to wavelet functions ($\langle \varphi_{j,k}(x), \psi_{j,k}(x)\rangle = 0$ for $k \neq l$). N-point Discrete Wavelet Transform of a function $f(x)$ can be written as in the equations (4) to (6) [29]:

$$f(x) = \frac{1}{\sqrt{N}}\left[\sum_{k=0}^{2^j-1} T_\varphi(j_0,k)\varphi_{j_0,k}(x) + \sum_{j=0}^{J-1}\sum_{k=0}^{2^j-1} T_\psi(j,k)\psi_{j,k}(x)\right] \tag{4}$$

$$T_\varphi(j_0,k) = \langle f(x), \varphi(x)\rangle = \frac{1}{\sqrt{N}}\sum_0^{N-1} f(x)\widetilde{\varphi(x)} \tag{5}$$

$$T_\psi(j,k) = \langle f(x), \psi_{j,k}(x)\rangle = \frac{1}{\sqrt{N}}\sum_0^{N-1} f(x)\widetilde{\psi_{j,k}(x)} \tag{6}$$

The functions $T_\varphi(j_0,k)$ are called scaling or approximation/low frequency coefficients and $T_\psi(j,k)$ are called wavelet or detail/high frequency coefficients, $\widetilde{\varphi(x)}$ and $\psi_{j,k}(x)$ are the duals of $\varphi(x)$ and $\psi(x)$. The Wavelet Transform is a powerful and right tool for approximating and analyzing one-dimensional piecewise smooth signals. Thanks to the separable extension from 1-D bases, it can isolate the discontinuities at edge points for images. However, its performance degrades for contours or curvilinear singularities, therefore directional representational transforms such as contourlets and shearlets are introduced [25], [26]. Contourlet Transform uses non-separable filterbank approach in order to capture and represent the directional information present in the images. There are mainly two parts to obtain the Contourlet Transform representation of an image. In the first part, the image is decomposed into sub-bands by using Laplacian Pyramid and point discontinuities in the sub-band decomposition stage are captured. In the second part, the details of the image are analyzed by directional filter banks [25]. Shearlet Transform detects image saline features such as directional singularities and geometrical features by defining the direction using shearing matrices. This transform forms an affine system by generating one single function which is dilated by a parabolic scaling and a shear matrix and translated in the time domain [26]. The multiscale of shearlets are obtained using A_a the parabolic scaling matrix and S_s the shear matrix for $a > 0$ and $s \in \mathbb{R}$ [26] and the resulting shearlet system is given by (7) and (8) :

$$A_a = \begin{pmatrix} a & 0 \\ 0 & \sqrt{a} \end{pmatrix} S_s = \begin{pmatrix} 1 & -s \\ 0 & 1 \end{pmatrix} \tag{7}$$

$$\left\{ \psi_{jkm}(x) = 2^{-j\frac{3}{2}}\psi\left(S_{-k}A_{4-j}x - m\right) : j, k \in \mathbb{Z}, m \in \mathbb{Z}^2 \right\} \tag{8}$$

where ψ is a shearlet, j, k and m denote the scale, shear and translation parameters, respectively. In this study, to see the practical perspective of these three sparsifying transforms, a synthetic image of letters O, G, R and S which have contours or curvilinear properties have been considered. The transform coefficients have been computed and depicted in Figure 1.
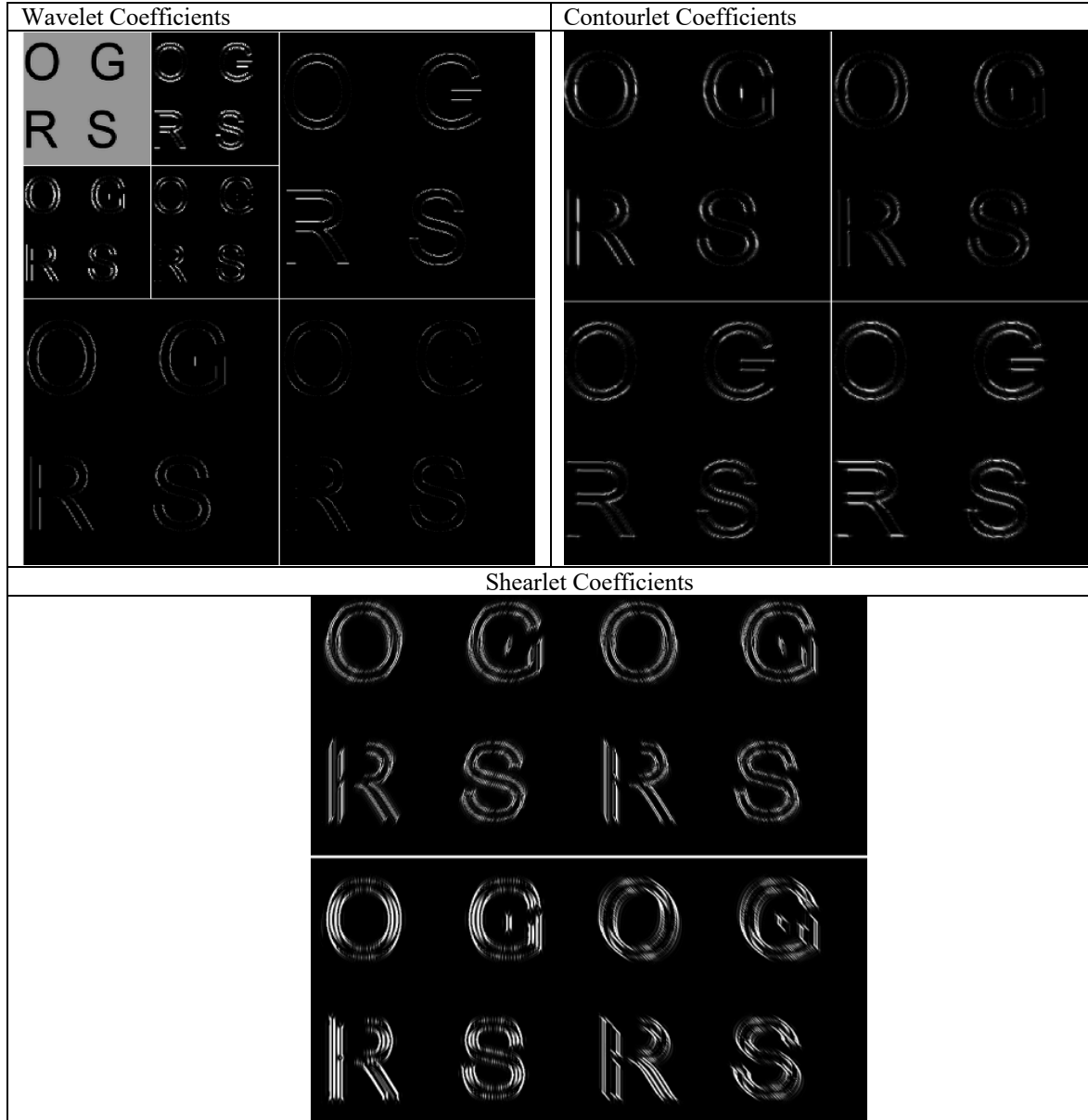
Figure 1. Wavelet, Contourlet and Shearlet Coefficients illustrations for letters O, G, R and S.

2.2 Alternating Direction Method of Multipliers (ADMM)

ADMM is a powerful convex optimization algorithm that combines the advantages of augmented Lagrangian and dual decomposition [18], [30]. ADMM is closely related to the Bregman iterative algorithms for ℓ_1 problems, proximal methods and Douglas–Rachford splitting algorithms in the literature. The algorithm is basically formed on a decomposition-coordination procedure with a goal to find a solution to a large scale problem by solving small local subproblems [18]. ADMM solves the following constrained optimization problem:

$$minimize\ f_1(x) + f_2(x)\ subject\ to\ Ax + By = c \tag{9}$$

where $x \in \mathbb{R}^n$, $y \in \mathbb{R}^m$, $A \in \mathbb{R}^{p \times n}$, $c \in \mathbb{R}^p$, f_1, f_2 are convex functions. As it is seen, the main difference of (9) from the general linear equality-constrained problem is that the variables have been split into two parts. The problem in (9) takes the form in (10) for compressed sensing or lasso or our image reconstruction problem:

$$minimize\ \tau\|z - Mx\|_2^2 + \|y\|_1\ subject\ to\ y = \Phi x \tag{10}$$

where z are measurements, M is masking operator and Φ is the sparsifying operator which is Wavelet, Contourlet or Shearlet Transform in our study. There are three main steps in ADMM: x-minimization step, y-minimization step and dual variable update. As the name of ADMM implies, the variables x and y are updated in an *alternating* manner [18]. The steps of ADMM of the convex minimization problem in (10) can be expressed as in the equations (11) to (13):

x-minimization step:

$$x^{k+1} = argmin_x\ \tau\|z - Mx\|_2^2 + \frac{\rho}{2}\|y^k - \Phi x + u^k\|_2^2 \tag{11}$$

y-minimization step:

$$y^{k+1} = argmin_y\ \|y\|_1 + \frac{\rho}{2}\|y - \Phi x^{k+1} + u^k\|_2^2 \tag{12}$$

dual variable update step:

$$u^{k+1} = u^k + y^{k+1} - \Phi x^{k+1} \tag{13}$$

where u is the dual variable and the penalty parameter $\rho > 0$.

3. Results

By using CS scheme, we have reconstructed peppers and Breast Cancer digital pathology image taken from TCGA [31] under different sparsifying transforms with MATLAB. As it is stated, Wavelet, Contourlet and Shearlet Transforms are used as sparsifying bases and the compression ratio is 8, in other words, 12.5 % of the pixels in the ground truth is used for reconstruction. The original and reconstructed images for 512×512 peppers and digital pathology image are given in Figure 2 and Figure 3 respectively.
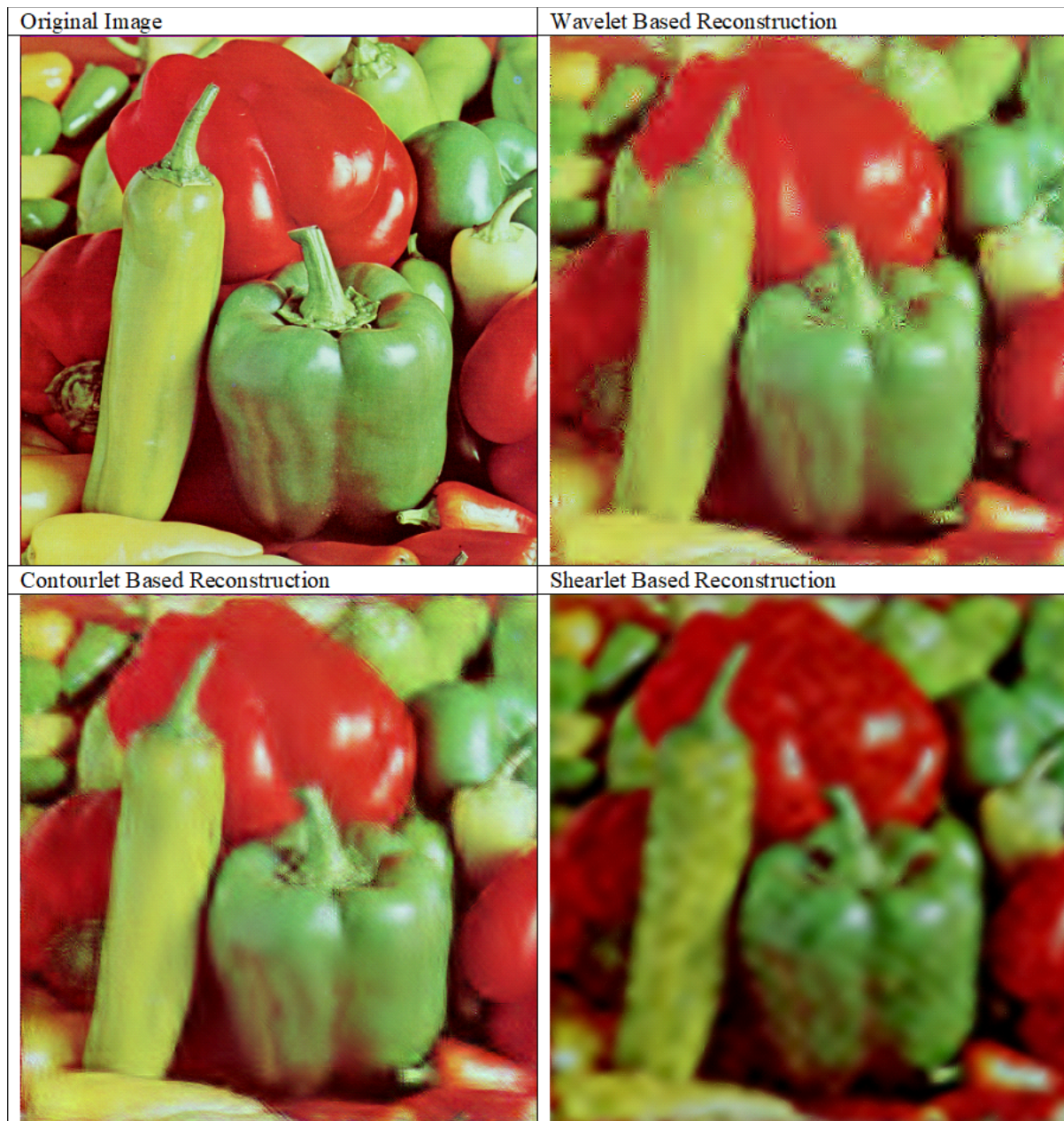
**Figure 2.** Peppers Image Reconstruction 512×512.
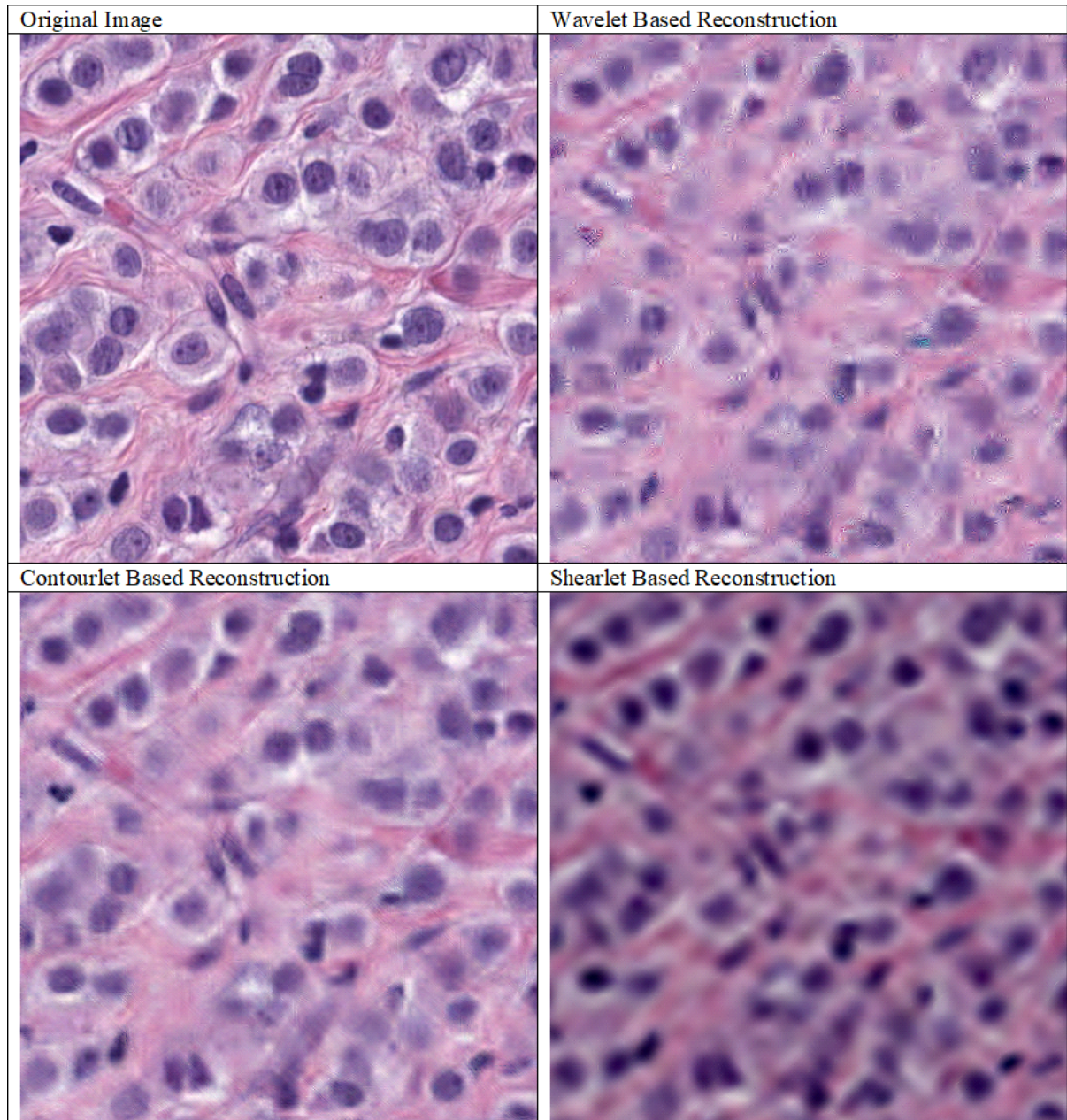
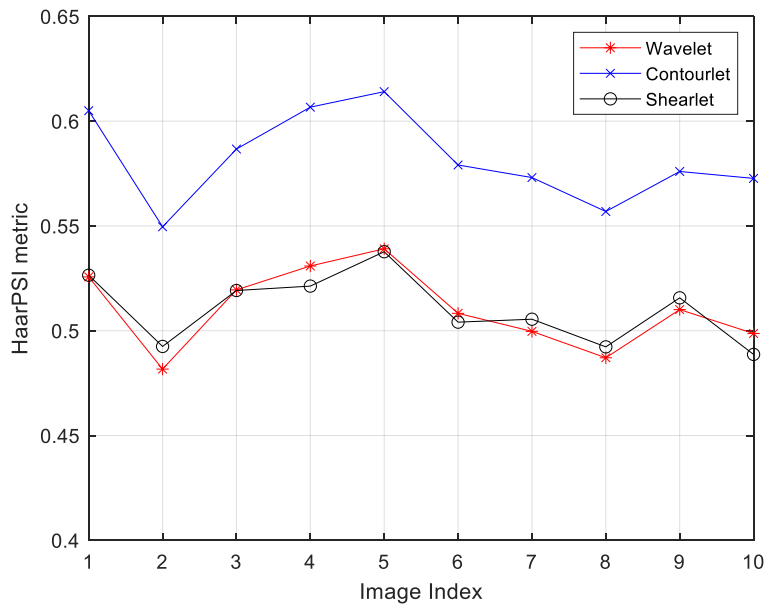**Figure 3.** Digital Pathology Image Reconstruction 512×512.

The quality of the reconstructed images are evaluated using reference based Image Quality Assessment (IQA) methods, namely SSIM [20] , HaarPSI [21] and PSNR. SSIM basically compares local patterns of pixel intensities that have been normalized for luminance and contrast [20]. On the other hand, HaarPSI makes decomposition with Haar wavelet to assess local similarities between two images and the obtained coefficients are utilized to make image comparison [21]. The calculated SSIM, HaarPSI and PSNR metrics for the reconstructed images are given Table 1. In order to investigate the performance of CS in digital pathology images profoundly, 10 different 512×512 images are extracted from different Breast Cancer whole slide images. After the reconstruction process, SSIM and HaarPSI metrics are calculated for each image, they are given Figure 4 and Figure 5 respectively.

Table 1. SSIM and HaarPSI metrics for Peppers and Digital Pathology Image.

Transform Type	Peppers			Digital Pathology Image		
	SSIM	HaarPSI	PSNR	SSIM	HaarPSI	PSNR
Wavelet	0.659	0.516	70.27	0.551	0.526	70.71
Contourlet	0.688	0.599	72.47	0.628	0.605	72.63
Shearlet	0.588	0.503	63.51	0.518	0.527	63.00
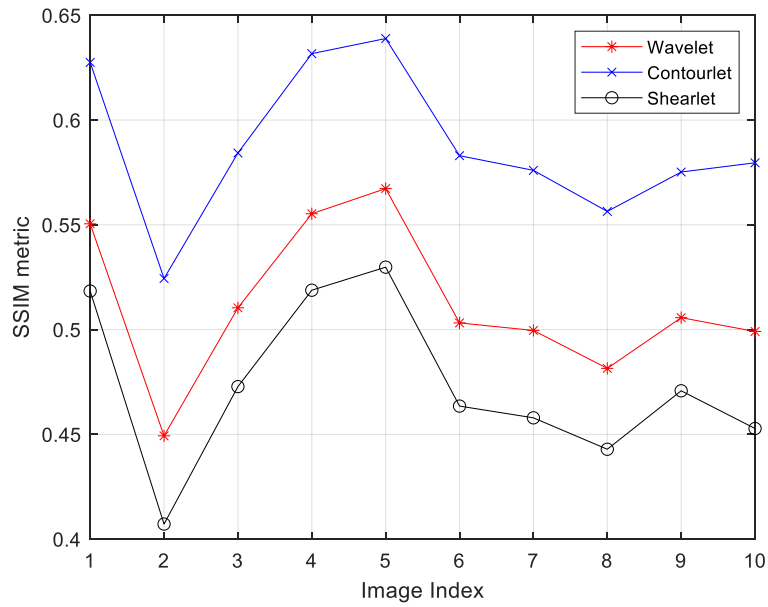
Figure 4. SSIM metrics for 10 different digital pathology images.

Figure 5. HaarPSI metrics for 10 different digital pathology images.

4. Discussion

In this research, compressed sensing with different sparsifying bases is considered specifically for digital pathology image. Figure 2 and Figure 3 show that the reconstruction is successful even when a few percent of the data (12.5 % for this particular case) is used. The quality measures changes for SSIM, HaarPSI and PSNR, however, if Table 1 is considered, it is seen that the performance of Contourlet Transform is better than Wavelet and Shearlet Transforms in every metrics. This observation aligns with the findings presented in Figure 1, which displays the transforms of synthetic image letters O, G, R, and S. These letters, characterized by their smooth curves and contours, serve as an effective analogy for the patterns and cellular structures typically observed in digital pathology images. In this context, the Contourlet Transform demonstrates a distinct advantage. Not only does it yield a sparse representation, but it also more accurately captures the edges, curves, and contours of these letters compared to both the Wavelet and Shearlet Transforms. This is clearly illustrated in Figure 1. The Contourlet Transform is particularly effective at showing smooth contours and continuous edges in images. It smoothly handles different levels of detail, allowing for a clearer and more accurate depiction of complex patterns. This feature is especially useful in digital pathology, where images often contain detailed and complicated structures.

During the study, it is observed that the fastest computation of coefficients is for the wavelet case. However, Contourlet Transform is faster to compute than Shearlet Transform, even though both transforms are considered as multilevel and multi resolution, the filter bank approach in Contourlet Transform is advantageous for the speed of computation. Besides, the reconstructions of digital pathology image are satisfactory compared to the reconstructions of classical peppers image when SSIM, HaarPSI and PSNR metrics are taken as a reference. While Table 1 shows that our reconstructions exhibit high quality based on PSNR values exceeding 40 dB, this metric does not accurately reflect the true quality of our images. This discrepancy arises because PSNR is traditionally geared towards grayscale images and may not correlate well with human visual perception, particularly in the context of color nuances and high dynamic range images. Figures 4 and 5 demonstrate the effectiveness of the Contourlet Transform, showcasing its application in 10 varied digital pathology images. In these figures, we have primarily focused on the results obtained from SSIM and HaarPSI measurements, which offer a more accurate and perceptually relevant assessment of image quality compared to PSNR. However, Wavelet and Shearlet Transforms result in similar quality in reconstruction specifically when the HaarPSI metric is taken into account. Digital pathology slide images can be more challenging than classical images, on the other hand, the results show that CS is very promising for digital pathology which is a growing medical industry. CS can be advantageous for imaging at different wavelengths; therefore, this study can initiate CS based imaging of digital pathology samples beyond the visible band.

Acknowledgements

References

[1] Jahn S, Plass M, and Moinfar F. "Digital Pathology: Advantages, Limitations and Emerging Perspectives," J. Clin. Med., vol. 9, p. 3697, Nov. 2020, doi: 10.3390/jcm9113697.

[2] Elgendi M, Fletcher RR, Abbott D, Zheng D, Kyriacou P, and Menon C, "Editorial: Mobile and wearable systems for health monitoring," Front. Digit. Health, vol. 5, 2023, doi: 10.3389/fdgth.2023.1196103.

[3] Freire D, de Faria P, Travençolo B, and Zanchetta do Nascimento M. "Automated detection of tumor regions from oral histological whole slide images using fully convolutional neural networks," Biomed. Signal Process. Control, vol. 69, p. 102921, Aug. 2021, doi: 10.1016/j.bspc.2021.102921.

[4] Joshi B, "Digital Pathology Market Size, Share, Trends Analysis Report by Application (Academic Research, Disease Diagnosis), by Product (Software, Device), by End-use (Diagnostic Labs, Hospitals), and Segment Forecasts, 2022-2030." 2022.

[5] Shannon CE, "A Mathematical Theory of Communication," Bell Syst. Tech. J., vol. 27, no. 3, pp. 379–423, 1948, doi: https://doi.org/10.1002/j.1538-7305.1948.tb01338.x.

[6] Taubman D and Marcellin M. JPEG2000 Image Compression Fundamentals, Standards and Practice. Springer Publishing Company, Incorporated, 2013.

[7]   Donoho DL, "Compressed sensing," IEEE Trans. Inf. Theory, vol. 52, no. 4, pp. 1289–1306, 2006, doi: 10.1109/TIT.2006.871582.

[8]   Candes EJ, , and Tao T. "Stable signal recovery from incomplete and inaccurate measurements," Commun. Pure Appl. Math., vol. 59, no. 8, pp. 1207–1223, 2006, doi: https://doi.org/10.1002/cpa.20124.

[9]   Candes EJ, J. R Romberg JK, and Tao T. "Robust uncertainty principles: exact signal reconstruction from highly incomplete frequency information," IEEE Trans. Inf. Theory, vol. 52, no. 2, pp. 489–509, 2006, doi: 10.1109/TIT.2005.862083.

[10] Graff C and Sidky E. "Compressive sensing in medical imaging," Appl. Opt., vol. 54, pp. C23-44, Mar. 2015, doi: 10.1364/AO.54.000C23.

[11] Lustig M, Donoho D, and Pauly JM, "Sparse MRI: The application of compressed sensing for rapid MR imaging," Magn. Reson. Med., vol. 58, no. 6, pp. 1182–1195, 2007, doi: https://doi.org/10.1002/mrm.21391.

[12] Bell J. "FDA Clears Compressed Sensing MRI Acceleration Technology From Siemens Healthineers." 2017.

[13] Radwell N, Mitchell K, Gibson G, Edgar M, Bowman R, and Padgett M. "Single-pixel infrared and visible microscope," Optica, vol. 1, pp. 285–289, Oct. 2014, doi: 10.1364/OPTICA.1.000285.

[14] Hahamovich E, Monin S, Hazan Y, and Rosenthal A. "Single pixel imaging at megahertz switching rates via cyclic Hadamard masks," Nat. Commun., vol. 12, Jul. 2021, doi: 10.1038/s41467-021-24850-x.

[15] Calisesi G. et al., "Compressed sensing in fluorescence microscopy," Prog. Biophys. Mol. Biol., vol. 168, pp. 66–80, 2022, doi: https://doi.org/10.1016/j.pbiomolbio.2021.06.004.

[16] Binev P, Dahmen W, DeVore R, Lamby P, Savu D, and Sharpley R. "Compressed Sensing and Electron Microscopy," in Modeling Nanoscale Imaging in Electron Microscopy, T. Vogt, W. Dahmen, and P. Binev, Eds., Boston, MA: Springer US, 2012, pp. 73–126. doi: 10.1007/978-1-4614-2191-7_4.

[17] Pavillon N, and Smith NI. "Compressed sensing laser scanning microscopy," Opt Express, vol. 24, no. 26, pp. 30038–30052, Dec. 2016, doi: 10.1364/OE.24.030038.

[18] Boyd S, Parikh N, Chu E, Peleato B, and Eckstein J. "Distributed Optimization and Statistical Learning via the Alternating Direction Method of Multipliers," Found. Trends Mach. Learn., vol. 3, pp. 1–122, Jan. 2011, doi: 10.1561/2200000016.

[19] Şengün Ermeydan E, Değirmenci A, Çankaya I, and Erdoğan F. "The Effects of Measurement Matrix and Reconstruction Algorithms on Compressed Sensing of Pathology Images," Düzce Üniversitesi Bilim Ve Teknol. Derg., vol. 8, no. 1, pp. 880–890, 2020, doi: 10.29130/dubited.626880.

[20] Wang Z, Bovik AC, Sheikh HR, and Simoncelli EP. "Image quality assessment: from error visibility to structural similarity," IEEE Trans. Image Process., vol. 13, no. 4, pp. 600–612, 2004, doi: 10.1109/TIP.2003.819861.

[21] Reisenhofer R, Bosse S, Kutyniok G, and Wiegand T. "A Haar wavelet-based perceptual similarity index for image quality assessment," Signal Process. Image Commun., vol. 61, pp. 33–43, 2018, doi: https://doi.org/10.1016/j.image.2017.11.001.

[22] Candes EJ, "The restricted isometry property and its implications for compressed sensing," Comptes Rendus Math., vol. 346, no. 9, pp. 589–592, 2008, doi: https://doi.org/10.1016/j.crma.2008.03.014.

[23] Baraniuk R, Davenport M, DeVore R, and Wakin M. "A Simple Proof of the Restricted Isometry Property for Random Matrices," Constr. Approx., vol. 28, pp. 253–263, Dec. 2008, doi: 10.1007/s00365-007-9003-x.

[24] Daubechies I. Ten Lectures on Wavelets. USA: Society for Industrial and Applied Mathematics, 1992.

[25] Do MN and Vetterli M. "The contourlet transform: an efficient directional multiresolution image representation," IEEE Trans. Image Process., vol. 14, no. 12, pp. 2091–2106, 2005, doi: 10.1109/TIP.2005.859376.

[26] Kutyniok G and Sauer T. "Adaptive Directional Subdivision Schemes and Shearlet Multiresolution Analysis," SIAM J. Math. Anal., vol. 41, pp. 1436–1471, Jan. 2009, doi: 10.1137/08072276X.

[27] Mallat SG, "A theory for multiresolution signal decomposition: the wavelet representation," IEEE Trans. Pattern Anal. Mach. Intell., vol. 11, no. 7, pp. 674–693, 1989, doi: 10.1109/34.192463.

[28] Meyer Y. Wavelets and Operators, vol. 1. in Cambridge Studies in Advanced Mathematics, vol. 1. Cambridge University Press, 1993. doi: 10.1017/CBO9780511623820.

[29] Gonzalez RC and Woods RE. Digital image processing. Upper Saddle River, N.J.: Prentice Hall, 2008. [Online]. Available: http://www.amazon.com/Digital-Image-Processing-3rd-Edition/dp/013168728X

[30] Bauschke HH, Burachik RS, Combettes PL, Elser V, Luke DR, and Wolkowicz H. Fixed-Point Algorithms for Inverse Problems in Science and Engineering. Springer Publishing Company, Incorporated, 2013.

[31] Gutman DA et al. "Cancer digital slide archive: An informatics resource to support integrated in silico analysis of TCGA pathology data," J. Am. Med. Inform. Assoc. JAMIA, vol. 20, no. 6, pp. 1091–1098, 2013, doi: 10.1136/amiajnl-2012-001469.